FARADAY

# Electric field-induced shifts of vibrational frequencies of CO adsorbed on Ni, Pd, Pt, Cu, Ag and Au metal (100) surfaces

## A theoretical comparative study

**Meng-Sheng Liao* and Qian-Er Zhang**

*State Key Laboratory for Physical Chemistry of Solid Surfaces, Chemistry Department, Xiamen University, Xiamen 361005, People's Republic of China*

A theoretical comparative study of electric field($F$)-induced vibrational frequency shifts of CO adsorbed on Ni, Pd, Pt, Cu, Ag and Au metal (100) surfaces is presented. The calculated vibrational tuning rates $d\omega_{C-O}/dF$ for the various metals are similar, thereby corroborating the experimental results of Ikezawa *et al.* The calculated absolute values are close to Lambert's observed values for CO on Ni in ultrahigh vacuum (UHV). The resulting estimates of the vibrational tuning rate with potential $V$ are in qualitative agreement with experimental data in aqueous electrolytes. The small experimental value of tuning rate for CO on Pt in UHV is not supported by the calculation. The M—CO bonding properties and their trends among the metals are also investigated.



## 1 Introduction

The vibrational frequencies of adsorbed species (ligand) on metal electrodes are shifted with an electric potential ($V$) is applied and this is regarded as one of the most interesting phenomena occurring in electrochemical adsorption processes. A number of electrochemical studies have been carried out for $CN^-$ adsorbed on coinage metal electrodes,[1] and CO adsorbed on Pt electrodes (Table 1). Experiments in UHV were carried out for CO on Ni(110), Ni(100) and Pt(111), where the vibrational frequency of CO on the surfaces varies with applied electrostatic field ($F$). The observation of the frequency shifts has also stimulated a variety of theoretical investigations. The shifts in vibrational frequencies of $CN^-$/Ag and CO/Pt due to an applied electrode potential ($V$) were studied by Anderson and co-workers[17,18] using a semiempirical ASED-MO (the atom superposition and electron delocalization molecular orbital) method. Bagus *et al.*[19–23] performed a series of *ab initio* cluster calculations for $CN^-$/Cu, CO/Cu and CO/Pd in the presence of an external electric field ($F$). Holloway and Nørskov[24] performed a model calculation for CO/Pt using a density-functional method. Another model calculation for CO/Pt was carried out by Korzeniewski *et al.*[25] All these calculations give a proper explanation for the observed potential- (or field-)dependent frequency shifts. Among these authors, however, controversy exists concerning

**Table 1** Experimental frequency ($\omega$) shifts with electrode potential ($V$) or electric field ($F$), for saturation coverage of CO terminally bonded to various metals in aqueous electrolytes or in UHV

| ref. | metal | electrolyte | $d\omega/dV$ / $cm^{-1}\ V^{-1}$ | $d\omega/dF$ / $10^6\ cm^{-1}\ V^{-1}\ cm$ |
|---|---|---|---|---|
| 2 | Pd(on-top) | 1 M $HClO_4$ | 48 | (1.71)[a] |
| 3 | Pt | 0.25 M HCOOH + 0.25 M $H_2SO_4$ | 28 | |
| 4 | Pt | 5 M $CH_3OH$ + 1 M $HClO_4$ | 30 | (1.07)[a] |
| 5 | Pt | 1 M $HClO_4$ | 35 | (1.25)[a] |
| | | 1 M $H_2SO_4$ | 24 | (0.86)[a] |
| 6 | Pt | 1 M $HClO_4$ | 30 | |
| | | 1 M $H_2SO_4$ | 30 | |
| | | 1 M HCl | 30 | |
| 7 | Pt | 0.25 M $H_2SO_4$ | 30 | |
| 8 | Au | 1 M $HClO_4$ | 64 | (2.29)[a] |
| | | 0.2 M NaOH | 64 | |
| | | 0.2 M $(CH_3)_4NOH$ | 64 | |
| 9 | Au | 0.1 M $HClO_4$ | 50 | (1.79)[a] |
| | | 0.1 M $NaClO_4$ | 50 | |
| 10 | Pt, Pd, Au, Ag | 0.1 M $NaClO_4$ | ~ 50 | |
| 11 | Pt(100) | 0.1 M $HClO_4$ | 36(high CO cov.) 48(low CO cov.) | |
| | Pt(111) | 0.1 M $HClO_4$ | 34(high CO cov.) 44(low CO cov.) | (1.57)[a] |
| | Pt(110) | 0.1 M $HClO_4$ | 30(high CO cov.) 30(low CO cov.) | |
| 12 | Ni(110) | (in UHV) | | 1.1 ± 0.4 |
| 13 | Ni(100) | (in UHV) | | 1.3 |
| 14 | Ni(100) | (in UHV) | | 1.4 ± 0.3 |
| 15,16 | Pt(111) | (in UHV) | | 0.34 ± 0.09 |

[a] Derived $d\omega/dF$ values according to eqn. (3).

the mechanism for the effect of electric fields on ligand–metal bonding. One interpretation assumes that the electric field changes the metal to ligand (CO or $CN^-$) π donation, which changes the number of antibonding π electrons on CO and results in the observed frequency shift. This is a chemical effect. The other interpretation is based on a dipole–field electrostatic interaction argument. According to this mechanism, the frequency shifts are determined by the interaction between the ligand dipole moment and the external field. This is a physical effect or Stark effect. Therefore, both chemical and physical effects may be used to explain observed frequency shifts of adsorbed ligands. Recently, Head-Gordon and Tully[26] investigated the connection of the chemical changes to the Stark effect model and show that similar chemical changes are in fact implicit in the Stark model. Lambert[14] had pointed out that the two explanations are equivalent and that either is correct. These viewpoints should resolve the question of the effect of external electric field on ligand–metal bonding.

The experimental situations for the shift of adsorbed CO vibrational frequency with electrode potential are given in Table 1. There is a large diversity in the experimental data for CO/Pt. From the earlier measurements in acidic solutions, estimates of the frequency shift for CO/Pt are *ca.* 30 $cm^{-1}$ $V^{-1}$, which is notably smaller than the value of 48 $cm^{-1}$ $V^{-1}$ reported for CO/Pd. For CO/Au, there are two contradictory experimental results, 64 and 50 $cm^{-1}$ $V^{-1}$. Later, Ikezawa *et al.*[10] performed a comparative study of the IR spectra of CO adsorbed on Pt, Pd, Au and Ag electrodes in a neutral electrolyte and found that all these electrodes show similar frequency shifts which are *ca.* 50 $cm^{-1}$ $V^{-1}$. More recently, Weaver *et al.*[11] reported a series of studies of the vibrational spectra of CO on ordered Pt electrodes. They showed that the $d\omega/dV$ value is sensitive to crystal surface orientation and is also coverage-dependent. Table 1 also gives the UHV results for vibrational frequency shift of CO adsorbed on Ni and Pt with electric field ($F_{local}$). For CO on Ni, the measured $d\omega/dF$ in vacuum is seen to be consistent with $d\omega/dV$ observed in electrolytes for CO on other metals. However, the difference in $d\omega/dF$ between Ni and Pt is surprisingly large. On the other hand, the vibrational tuning rate for CO on Pt(111) is seen to be much smaller in UHV than it is in electrochemical cells.

Because the magnitude of the vibrational frequency shift of the adsorbed ligand may be affected by various factors (type of electrolyte, coverage *etc.* and also the potential region), it is hard to say which sets of experimental data are more reliable. Further experiments are desirable, to ascertain whether or not the marked potential-(or field) dependent behaviour is the same on the different metals in a similar environment. Here, we attempt to perform a theoretical comparative study of CO adsorbed on Ni, Pd, Pt, Cu, Ag and Au metals in the presence of an uniform electric field. Calculations on these systems would be of interest to determine whether there is any variation in $d\omega/dF$ with different metals. It may be assumed that the difference in $d\omega/dV$ could be caused by a difference in $d\omega/dF$. Another aim is to find theoretical values of $d\omega/dV$. To date, no experiments have been carried out for CO/Cu, either in an electrochemical cell or in UHV. In addition to the $d\omega_{C-O}/dF$ behaviour, we also investigate some related properties.

## 2 Computational details

Our calculations were carried out using the ADF (Amsterdam density functional) program developed by Baerends *et al.*[27] Triple ζ STO basis sets are employed for the metal $(n-1)$d–*n*s as well as the C and O 2s–2p valence shells. Single-ζ STOs are used for core orthogonalization. Polarization functions have been added to the valence bases: one p-type polarization function for the metals and one d-type polarization function for C and O. The other shells of lower energy, *i.e.* [He] for C and O, [Ar] for Ni and Cu, [Kr] for Pd and Ag and [Xe $4f^{14}$] for Pt and Au, were considered as core shells and kept frozen according to the frozen-core technique.[27] Two types of DF approximations were used: the Vosko, Wilk and Nusair local spin-density potential[28] (labelled VWN) and one including the non-local gradient exchange and correlation corrected potentials due to Becke[29] and Perdew[30] (labelled VWN–B–P). It was shown that the VWN–B–P functional could give accurate binding energies for both main-group and transition-metal systems.[31,32] However, we found that the calculations with the non-local corrections yield an infinite M—CO bond expansion for the weakly bound $Ag_{10}$—CO and $Au_{10}$—CO systems. Hence, we employed the VWN potential for the two systems. For the other systems, both VWN and VWN–B–P potentials were used. The relativistic corrections are calculated by the quasi-relativistic method.[33]

We choose metal M(100) as the surface for adsorption, and M(100) is imitated by a square pyramid $M_{10}(5, 4, 1)$ cluster which contains five atoms in the first layer, four in the second and one in the third. The CO molecule is placed vertically at the on-top site of the cluster with the C end down to the surface. This adsorption geometry is supported by experimental evidence for CO on various metals.[34]

In the presence of an external field *F*, the Hamiltonian is given by

$$H(F) = H_{DF}(F=0) + \boldsymbol{F}\cdot\left(\sum_i \boldsymbol{r}_i - \sum_A Q_A \boldsymbol{R}\right) \quad (1)$$

where $H_{DF}(F=0)$ is the field-free Hamiltonian; $\boldsymbol{r}_i$ and $\boldsymbol{R}_A$ are the electron and nuclear coordinates, respectively; $Q_A$ is the nuclear charge. If the last term in eqn. (1) is treated by first-order perturbation theory, the total perturbation energy is then given by

$$E_P = E_{DF}(F=0) - \boldsymbol{\mu}(F=0)\cdot\boldsymbol{F} \quad (2)$$

Here $E_{DF}(F=0)$ is the energy of the system for $F=0$ and $\mu(F=0)$ is the dipole moment of $M_{10}$—CO. So the term $\boldsymbol{\mu}(F=0)\cdot\boldsymbol{F}$ represents the electrostatic interaction of an external electric field with the adsorbed CO dipole. In the calculations, the electric field *F* is assumed to be uniform and we have chosen $F = \pm 0.01$ a.u. $= 5.14\times10^{-7}$ V $cm^{-1}$. The magnitude of this field is believed to be comparable to the fields on the electrode surface of an electrochemical cell when a potential of 1 V is applied.[19,20] Bagus *et al.*[19–23] described the ωs obtained with the $E_P$ energy surface as Stark frequencies and the ωs obtained with the $E_{SCF}$ energy surface as SCF frequencies. All their calculations demonstrated that the difference between the results obtained by the perturbative approach and by the full variational SCF method is small. This is also justified by our ADF calculations on CO/Cu and isolated CO. An explanation for this behaviour is given by Head-Gordon and Tully.[26] Thus, for CO adsorbed on the other metals we have only determined the perturbation theory energies $E_P$ and the properties derived from them.

## 3 Results and Discussion

### 3.1 Isolated CO

We have performed a calculation on isolated CO in a uniform electric field. Isolated CO is the reference point for discussing the effect of electric field on adsorbed CO. The calculated results (bond length, bond energy *etc.*) with both VWN and VWN–B–P potentials are given in Table 2, together with experimental and previous theoretical data.

We will first discuss the results for $F=0$ (*i.e.* without field). The bond length calculated with the VWN potential is very close to the experimental value, the error being 0.002 Å. The VWN–B–P potential overestimates the bond length by 0.011 Å.

**Table 2** Calculated molecular properties[a] of CO in uniform electric field of $F = 0$ and $\pm 0.01$ a.u.

| | | $R_e$ | $D_e$ | $k_e$ | $\omega_e$ | $\mu^b$ |
|---|---|---|---|---|---|---|
| $F = 0$ | VWN | 1.130 | 12.88 | 18.99 | 2166 | 0.174 |
| | VWN–B–P | 1.139 | 11.85 | 18.01 | 2109 | 0.174 |
| | CASSCF[c] | 1.138 | | | 2147 | 0.30 |
| | HF[d] | 1.117 | | | 2424 | −0.179 |
| | HF[e] | 1.135 | | | 2267 | |
| | exp. (ref. 37) | 1.128 | 11.22 | | 2170 | 0.1222 |
| $F = +0.01$ | VWN (P) | 1.127(−0.003) | | 19.41 | 2190(24) | |
| | VWN (SCF) | 1.127 | | 19.43 | 2191 | |
| | VWN–B–P (P) | 1.136(−0.003) | | 18.40 | 2132(23) | |
| | CASSCF[c] | 1.136(−0.002) | | | 2165(18) | |
| | HF[d] | 1.114(−0.003) | | | 2455(31) | |
| | HF[e] | 1.131(−0.004) | | | 2302(35) | |
| $F = -0.01$ | VWN (P) | 1.134(0.004) | | 18.55 | 2141(−25) | |
| | VWN (SCF) | 1.134 | | 18.59 | 2143 | |
| | VWN–B–P (P) | 1.143(0.004) | | 17.47 | 2078(−31) | |
| | HF[d] | 1.121(0.004) | | | 2389(−35) | |
| | HF[e] | 1.139(0.004) | | | 2228(−39) | |

| | | |
|---|---|---|
| $(d\omega/dF)$ /$10^{-7}$ cm$^{-1}$ V$^{-1}$ cm | VWN (P) | 4.77 |
| | VWN–B–P (P) | 5.25 |
| | CASSCF[c] | 3.6 ($F$ = 0–0.01 a.u) |
| | HF[d] | 6.42 ($F = -0.01$–0.01 a.u.) |
| | HF[e] | 7.20 |
| | HF[f] | 6.0 |
| | exp.[g] | 4.28 ± 0.06 |

[a] Bond length $R$ in Å, bond energy $D_e$ in eV, force constant $k$ in N cm$^{-1}$, vibrational frequencies $\omega$ in cm$^{-1}$ and dipole moment $\mu$ in D. [b] Positive sign in $\mu$ corresponds to C$^-$—O$^+$. [c] CASSCF calculation by Bauschlicher.[35] [d] Hartree–Fock calculation by Andrés *et al.*[36] [e] Hartree–Fock calculation by Head-Gordon and Tully.[26] [f] Hartree–Fock calculation by Bagus and Pacchioni.[23] [g] Estimated by substituting experimentally measured moments into the third-order perturbation theory result.[14] The values in parentheses are the differences between the values for $F = 0$ and $F = \pm 0.01$ a.u., $P$ = perturbation; SCF = full SCF calculation.



On the other hand, the VWN potential gives a vibrational frequency that is much closer to experiment than does the VWN–B–P potential. However, the VWN potential yields a bond energy which is 1.7 eV (15%) too large. The inclusion of the non-local corrections reduces the bond energy by 1 eV and so remarkably improves the agreement between calculation and experiment. The experimental value of the dipole moment $\mu$ is well reproduced by the ADF calculation. The HF calculation does not give the correct sign for the dipole moment for free CO owing to neglect of electron correlation. The vibrational frequencies calculated at the HF level are also greatly overestimated compared with the experimental values.

Concerning the results for $F = \pm 0.01$ a.u., frequency shifts of 24 cm$^{-1}$ up and 25 cm$^{-1}$ down are obtained for the positive and negative fields, respectively. These frequency shifts lead to an average vibrational tuning rate of $d\omega/dF = 4.77 \times 10^{-7}$ cm$^{-1}$ V$^{-1}$ cm. At the VWN–B–P level, the rate of change is 7 cm$^{-1}$ less at positive field than at negative field, and the calculated tuning rate $d\omega/dF$ is $5.25 \times 10^{-7}$ cm$^{-1}$ V$^{-1}$ cm. The most recent experimental value of Lambert[14] for this quantity is $(4.28 \pm 0.06) \times 10^{-7}$ cm$^{-1}$ V$^{-1}$ cm. Thus, the VWN value is closer to the experimental value than the VWN–B–P value. Our ADF values are intermediate between the CASSCF and HF results. The C—O bond length $R$ is very weakly dependent on field. In Table 2, the bond length shifts ($\Delta^F R$) are less than 0.005 Å. The different calculational methods give similar $\Delta^F R$. The change $\Delta k$ in the C—O force constant induced by the field $F = \pm 0.01$ a.u. is $\pm 0.43$ N cm$^{-1}$. Hence, a very small change in the C—O bond length with field, is accompanied by a relatively large variation in the C—O force constant. One can see that the results obtained by the perturbative approach are very close to those obtained by the full variational SCF method.

### 3.2 Adsorbed CO

We now turn our attention to adsorbed CO. The $M_{10}$—CO system contains two types of bonds, M—CO and C—O. We first determine the M—CO and C—O bond lengths and force constants. An internal coordinate approach[22] is used. The calculations start from bond lengths $r_0$(M—CO) and $r_0$(C—O); these $r_0$s are chosen close to $r_e$. For the C—O vibration, the position of the ligand centre of mass is fixed and the C—O distance is varied. For the metal–CO vibration, the C—O distance is fixed and M—CO distance is varied. The energy calculations were carried out with step length $\Delta R = 0.1$ a.u. We fitted an $n$th degree polynomial to the lowest $m$ points ($m > n$) and found that reliable results can be obtained from the lowest nine points fitted by a fifth-degree polynomial. From this, the equilibrium values, $R_e$, were obtained and the stretching force constants, $k_e$, were calculated by using the second derivative of the energy with respect to the bond length at $R_e$. The internal coordinate approach neglects the coupling force constant of the two internal modes, which is expected to be small.[19–23] After obtaining $k_{M–CO}$ and $k_{C–O}$, we then set up the secular equation to determine the frequencies $\omega_{M–CO}$ and $\omega_{C–O}$ (the mass of the metal cluster is assumed to be infinite). In this case, the obtained frequencies are called the normal-mode frequencies, which involve a mixture of the internal M—CO and C—O modes.

**3.2.1 Metal–CO bonding.** The metal–CO bonding is often interpreted on the basis of the σ donation π backdonation mechanisms. Some detailed discussion for the picture of the bonding between CO and metal clusters can be found in the literature.[38–40] Here, we present our calculated properties for CO adsorbed on the various metals, before discussing the electric field effects on the vibrational frequencies. The results are given in Table 3.

First, we examine the adsorption energies. For the transition metals M = Ni, Pd and Pt, the adsorption energies calculated with the VWN potential are greatly overestimated (by 1.37, 0.66 and 1.16 eV, respectively) compared with the experimental data. (The adsorption properties for CO at the on-top site of Pt(100) and Pt(111) may be expected to be similar). The inclusion of the BP nonlocal corrections has a 1 eV effect and makes a significant improvement in the adsorption energies. The calculation gives the order in $E_{ads}$: Pd < Ni ≈ Pt, while

**Table 3** Calculated properties[a] for CO adsorbed at on-top site of the $M_{10}$ cluster

| | | $R_{M-CO}$ | $R_{C-O}$ | $E_{ads}$ | $k_{M-CO}$ | $k_{C-O}$ | $\omega_{M-CO}$ [b] | $\omega_{C-O}$ |
|---|---|---|---|---|---|---|---|---|
| M = Ni | VWN | 1.69 | 1.159 | 2.67 | 4.07 | 15.69 | 475 | 2055 |
| | VWN–B–P | 1.72 | 1.166 | 1.77 | 3.54 | 14.86 | 445 | 1993 |
| | exp[c] | | | 1.30[d] | | | 460*[e] | 2000[e] |
| | | | | | | | 480*[f] | |
| M = Pd | VWN | 1.85 | 1.150 | 2.22 | 3.29 | 16.50 | 432 | 2087 |
| | VWN–B–P | 1.90 | 1.157 | 1.35 | 2.67 | 15.75 | 391 | 2029 |
| | exp[g] | | 1.13 ± 0.01[h] | 1.56[i] | | | 340*[h] | 1895[j] |
| M = Pt | VWN | 1.83 | 1.149 | 2.59 | 4.54 | 16.84 | 501 | 2133 |
| | VWN–B–P | 1.86 | 1.159 | 1.71 | 3.77 | 15.83 | 459 | 2057 |
| | exp[k] | | | 1.43[l] | | | 480[m] | 2065[n] |
| | | | | | | | | 2090[m] |
| | | | | | | | | 2080[o] |
| M = Cu | VWN | 1.87 | 1.144 | 0.95 | 1.59 | 17.15 | 305 | 2090 |
| | VWN–B–P | 1.96 | 1.150 | 0.29 | 0.86 | 16.13 | 226 | 2014 |
| | exp[c] | 1.9 ± 0.1 | 1.15 ± 0.1[p] | 0.65[q] | | | 340[r] | 2079[s] |
| | | | | | | | 350[t] | 2078[u] |
| | | | | | | | 344[u] | |
| M = Ag | VWN | 2.19 | 1.135 | 0.42 | 0.50 | 18.08 | 173 | 2123 |
| | exp[k] | | | 0.26 | | | | |
| M = Au | VWN | 2.08 | 1.135 | 0.59 | 0.99 | 18.07 | 243 | 2132 |
| | exp[v] | | | | | | | 2111 |

[a] Bond length $R$ in Å, adsorption energy $E_{ads}$ in eV, force constant $k$ in N cm$^{-1}$ and vibrational frequencies $\omega$ in cm$^{-1}$. [b] The M—CO vibrational frequency seems to be insensitive to CO-coverage; it was shown that the observed M—CO vibrational frequency seems to be insensitive to CO-coverage; it was shown that the observed M—CO frequencies on Ni(111) and Pt(111) at low CO-coverage are same as those at high CO-coverage ($\theta_{CO} \approx 0.5$).[42] [c] For CO adsorbed at on-top site of M(100). [d] Ref. 41. [e] Ref. 42. [f] Ref. 43. [g] For CO adsorbed on two-fold bridging site of Pd(100). [h] Ref. 45. [i] Ref. 44. [j] Ref. 46. [k] For CO adsorbed at on-top site of M(111).[56] [l] Ref. 47. [m] Ref. 48. [n] Ref. 49. [o] Ref. 50. [p] Ref. 34. [q] Ref. 51. [r] Ref. 52. [s] Ref. 54. [t] Ref. 53. [u] Ref. 55. [v] For CO on polycrystalline gold surface.[57] The experimental frequencies are for low CO-coverage except those with *, where $\theta_{CO} \approx 0.5$.



the experimental $E_{ads}$ values show a different order: Pd > Ni ≈ Pt. This is because, experimentally, the preferred sites for CO adsorption are different for the different metals. On Ni(100) and Pt(111), CO favours binding to one-fold (on-top) sites; on Pd(100) it adsorbs on two-fold bridging sites. Here we consider an on-top site for M = Pd in the calculations. For CO adsorption on the coinage metals, the M—CO bonding is relatively weak. For M = Cu, where $E_{ads}^{exp} = 0.65$ eV, the calculation with the BP non-local corrections results in adsorption energies that are too small (by *ca.* 0.4 eV), whereas the $E_{ads}$ calculated with the VWN potential is somewhat too large (by 0.25 eV). For M = Ag, the calculated VWN value of 0.42 eV is in good agreement with the experimental value of 0.26 eV on Ag(111). No experimental adsorption energy is available for M = Au. The calculations with the non-local B–P corrections give zero adsorption energies for CO/Ag and CO/Au (no minimum is found in the $M_{10}$—CO binding energy curve). The ordering in the adsorption energies of CO on the coinage metals is: Cu > Au > Ag. The relativistic effects are responsible for the anomalous order from M = Ag to Au. A schematic illustration of the VWN adsorption energies is shown in Fig. 1. The calculations with non-local corrections do not change the order.

The C—O bond length is increased in the $M_{10}$CO by 0.005 Å (M = Au)–0.03 Å (M = Ni) with respect to free CO. The increase in $R_{C-O}$ has been attributed to metal backdonation to the antibonding CO 2π* orbital, which causes a weakening of the C—O bond. Corresponding to the C—O bond expansion, the C—O force constant decreases by 0.9–3.3 N cm$^{-1}$ and the C—O vibrational frequency is lowered by 30–110 cm$^{-1}$. The calculated C—O bond length with non-local corrections is *ca.* 0.01 Å longer. The M—CO distance is much more sensitive to the inclusion of the BP corrections, especially for the CO weakly bound systems. The calculated Cu—C distances are within 0.1 Å of the experimental value (1.9 ± 0.1 Å). Experimental C—O bond lengths for adsorbed CO are known for M = Cu and Pd. The calculated C—O bond lengths in $M_{10}$CO are shown to agree well with the experimental values.

Fig. 2 shows the variations in the VWN M—CO and C—O bond lengths with the metal. A larger $R_{M-CO}$ corresponds to a smaller $R_{C-O}$, indicating that π backdonation from M to CO 2π* is larger for smaller $R_{M-CO}$. The non-relativistic M—CO bond lengths are also shown in the figure. The shorter Pt—CO and Au—CO bond lengths as compared with the Pd—CO and Ag—CO values are due to relativistic effects. The relativistic effects are small on the ligand C—O bond length. The variations in the M—CO and C—O force constants are consistent with the trend of the calculated bond lengths (Fig. 3).

Let us look at the vibrational frequencies. The experimental M—CO and C—O vibrational frequencies ($\omega$), given in Table 3, are seen to be somewhat different for different authors. For M = Ni, experimental estimates of the $\omega_{Ni-CO}$ are 460 and 480 cm$^{-1}$. The calculated $\omega_{Ni-CO}$ value of 475 cm$^{-1}$ with the VWN potential is intermediate between them; the VWN–B–P value of 445 cm$^{-1}$ is underestimated. Compared with the experimental $\omega_{C-O}$ value of 2000 cm$^{-1}$, the VWN–B–P potential gives very good result (1993 cm$^{-1}$), while the VWN value is overestimated by 55 cm$^{-1}$. For M = Pd, the experimental

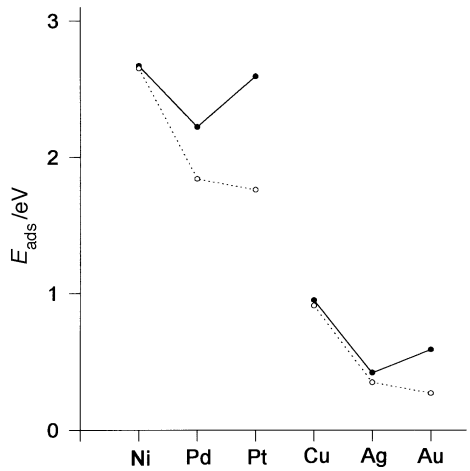


**Fig. 1** Schematic illustration of the calculated adsorption energies $E_{ads}$ for CO on different metals. The open circles represents the non-relativistic results.

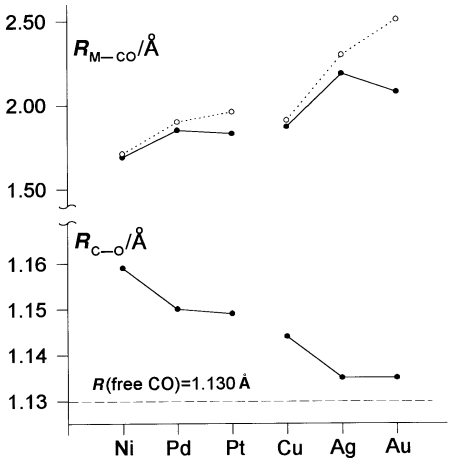


**Fig. 2** Schematic illustration of the calculated M—CO and C—O bond lengths $R$. The open circles represents the non-relativistic results.



vibrational frequencies have been assigned to CO adsorbed on bridging sites of Pd(100). The calculated frequencies for CO at on-top sites are found to be greatly overestimated, even with the VWN–B–P potential. For M = Pt, the VWN–B–P frequencies of Pt—CO and C—O are underestimated compared with the experimental data, while the VWN values are somewhat too large. For M = Cu, the VWN–B–P potential gives the Cu–CO frequency which is too small by more than 110 $cm^{-1}$ compared with the experimental data (340–350 $cm^{-1}$); the VWN–B–P value of $\omega_{C-O}$ (2014 $cm^{-1}$) is also underestimated by 65 $cm^{-1}$. Without including the non-local corrections, the calculated $\omega_{Cu-CO}$ and $\omega_{C-O}$ are 80 $cm^{-1}$ larger (compared with the VWN values) and so much closer to the experimental data. For M = Au, the experimental $\omega_{C-O}$ value was estimated for CO on a polycrystalline surface. The calculated C—O frequency compares well with the experimental value, the error being 21 $cm^{-1}$ (1%). No experimental data on the vibrational frequencies are known for M = Ag.

To summarize: For the transition metals, the VWN potential strongly overestimates the adsorption energies $E_{ads}$, on average by 1.3 eV. The non-local B–P correction to $E_{ads}$ is quite large (*ca.* −1 eV) and greatly improves the agreement between the calculations and experiment. The vibrational frequencies calculated with both VWN and VWN–B–P potentials are in good agreement with the experimental data. In general, the VWN values are somewhat overestimated while the VWN–B–P values are somewhat too low. For the coinage metals, the experimental adsorption energies are intermediate between the values calculated with the VWN and VWN–B–P potentials; concerning the frequencies, the VWN potential performs much better than the VWN–B–P potential.

Bertolini and Tardy[42] found a linear correlation between $(\omega_{M-CO})^2$ and $E_{ads}$ from experimental data. Therefore, one may suppose that $k_{M-CO}$ is proportional to $E_{ads}$. Fig. 4 shows the relation between the calculated $k_{M-CO}$ and $E_{ads}$; we see that there is a good linear relationship.

**3.2.2 Field-induced vibrational frequency shifts.** Table 4 shows the effects of electric fields on adsorbed CO on M(100), as modelled by cluster calculations. The magnitudes of the frequency shifts with respect to the field-free case ($F = 0$) are given separately in Table 5. From these data, we can determine the average vibrational tuning rate $d\omega^{av}/dF$ in the range of fields applied. The variation of the calculated C—O frequency with applied electric field is found to be nearly linear. The available experimental $d\omega/dF$ data in UHV were given in Table 1. In order to enable comparison of the calculated $d\omega/dF$ with the experimental data $d\omega/dV$, it is necessary to know the relation between an applied field, given in V $cm^{-1}$, and a potential, given in V, across the electrodes in an electrochemical cell. The transposition of the $d\omega/dF$ and $d\omega/dV$ values can be made using

$$\frac{d\omega}{dF} = \left(\frac{dF}{dV}\right)^{-1} \frac{d\omega}{dV} \quad (3)$$

According to Lambert,[13] $dF/dV$ may be approximated as the differential capacitance $C$ divided by the relative permittivity $\varepsilon$ (SI units)

$$\frac{dF}{dV} = \frac{C}{\varepsilon} \quad (4)$$

To determine $C$ and $\varepsilon$, one has to make some assumption about the structure of the electrochemical double layer.[13] For CO adsorbed on the Pt electrode, $\varepsilon$ was assumed to be $7\varepsilon_0$ at the electrode surface (where $\varepsilon_0$ is the vacuum relative permittivity = $8.85 \times 10^{-12}$ $J^{-1}$ $C^2$ $m^{-1}$), and the capacitance $C$ was found to be *ca.* 17 μF $cm^{-2}$. Thus, $dF/dV$ was found to be *ca.* $2.8 \times 10^7$ V $cm^{-1}$ $V^{-1}$.[13–16] The resulting $d\omega/dF$ values for the experimental data in aqueous electrolytes are given in Table 1. Although the conversion factor is given for CO/Pt, it may be used to estimate $d\omega/dF$ for CO on other metal electrodes.[14,22] It should be pointed out that the capacitance of the double layer might be different for different metals and the relative permittivity would depend on the electrolyte.

The $\omega_{C-O}$ shifts ($\Delta\omega$) induced by a field $F = \pm 0.01$ a.u. on the adsorbed CO are ±60–70 $cm^{-1}$, two or three times larger

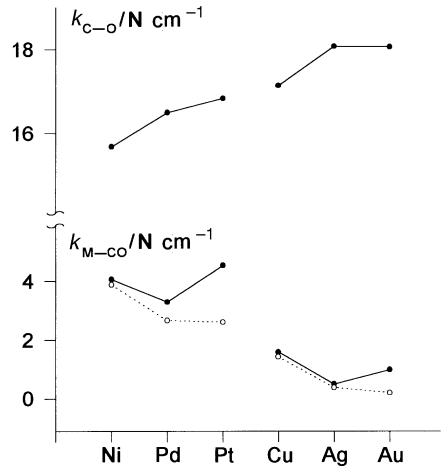


**Fig. 3** Schematic illustration of the calculated M—CO and C—O force constants. The open circles represents the non-relativistic results.

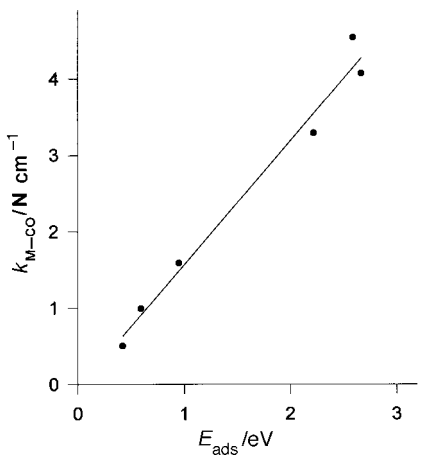


**Fig. 4** Relation between M—CO force constant $k_{M-CO}$ and adsorption energy $E_{ads}$.

**Table 4** Calculated properties[a] of $M_{10}CO$ in uniform electric fields of $F = \pm 0.01$ a.u.

| | $F = +0.01$ | $F = -0.01$ | $F = +0.01$ | $F = -0.01$ |
|---|---|---|---|---|
| | $R_{M-CO}$ | | $R_{C-O}$ | |
| M = Ni | 1.69(1.71) | 1.68(1.70) | 1.149(1.149) | 1.170(1.172) |
| M = Pd | 1.85(1.91) | 1.84(1.89) | 1.140(1.139) | 1.160(1.159) |
| M = Pt | 1.84(1.96) | 1.82(1.95) | 1.140(1.137) | 1.159(1.159) |
| M = Cu | 1.89(1.92) | 1.86(1.90) | 1.135(1.135) | 1.152(1.151) |
| SCF[b] | 1.89 | 1.87 | 1.136 | 1.153 |
| M = Ag | 2.22(2.33) | 2.15(2.27) | 1.128(1.127) | 1.143(1.143) |
| M = Au | 2.09(2.51) | 2.06(2.51) | 1.128(1.126) | 1.143(1.140) |
| | $k_{M-CO}$ | | $k_{C-O}$ | |
| M = Ni | 3.97(3.77) | 4.18(4.00) | 16.86(16.82) | 14.52(14.45) |
| M = Pd | 3.16(2.49) | 3.40(2.83) | 17.57(17.67) | 15.43(15.40) |
| M = Pt | 4.33(2.54) | 4.73(2.67) | 17.90(17.94) | 15.77(15.43) |
| M = Cu | 1.50(1.38) | 1.68(1.50) | 18.30(18.51) | 16.00(16.20) |
| SCF[b] | 1.54 | 1.63 | 18.29 | 15.87 |
| M = Ag | 0.45(0.37) | 0.58(0.41) | 19.18(19.38) | 16.96(16.89) |
| M = Au | 1.00(0.20) | 1.00(0.20) | 19.09(19.61) | 17.05(17.30) |
| | $\omega_{M-CO}$ | | $\omega_{C-O}$ | |
| M = Ni | 471(460) | 479(470) | 2122(2116) | 1987(1978) |
| M = Pd | 424(379) | 437(401) | 2146(2138) | 2025(2011) |
| M = Pt | 492(383) | 509(391) | 2189(2155) | 2075(2009) |
| M = Cu | 297(285) | 313(297) | 2155(2165) | 2022(2031) |
| SCF[b] | 301 | 309 | 2155 | 2014 |
| M = Ag | 164(149) | 186(156) | 2185(2194) | 2058(2051) |
| M = Au | 244(110) | 244(110) | 2190(2205) | 2072(2071) |

[a] Bond length $R$ in Å, force constant $k$ in N cm$^{-1}$ and vibrational frequencies $\omega$ in cm$^{-1}$. [b] Full SCF calculation for CO/Cu. The values in parentheses are the non-relativistic results.



than the shift calculated for the free CO. The bond length changes are twice as large. The difference between the $d\omega/dF$ values for adsorbed and free CO is mostly due to the increase in $|d\mu/dR_{C-O}|$. This can be elucidated by eqn. (2), together with Fig. 5, which shows the changes in $\mu$ with the C—O distance for $Cu_{10}CO$ and free CO. As Lambert did,[13] we make Taylor expansions of the molecular potential and the dipole moment in terms of the relative bond length $(R - R_e)$

$$E_{DF}(F = 0) = a_0 + a_2(R - R_e)^2 + a_3(R - R_e)^3 + \cdots \quad (5)$$

$$\mu(F = 0) = M_0 + M_1(R - R_e) + M_2(R - R_e)^2 + \cdots \quad (6)$$

The frequency $\omega$ shift with field $F$ is found to be[13]

$$\frac{d\omega}{dF} = \omega_e(F = 0)\frac{(3M_1 a_3 - 2a_2 M_2)}{4a_2^2} \quad (7)$$

From Fig. 5, there is a good linear relation between $\mu$ and $R$, namely $M_2 \approx 0$. Hence

$$\frac{d\omega}{dF} = \omega_e(F = 0)\frac{3M_1 a_3}{4a_2^2} \quad (8)$$

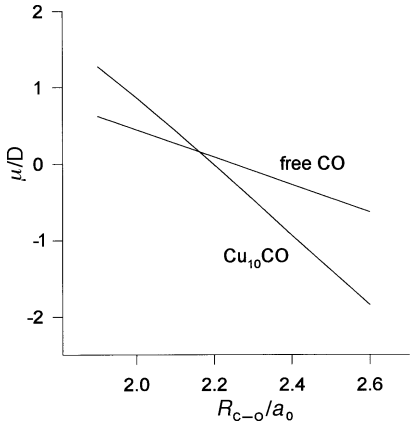


**Fig. 5** Changes in dipole moment $\mu$ with C—O distance $R_{C-O}$ for $Cu_{10}CO$ and free CO (the Cu—C distance is fixed at $R_e$ when C—O is varied).

Here, $M_1$ represents the slope $d\mu/dR$. So an increase in $|d\mu/dR|$ explains the larger change in $d\omega/dF$.

The VWN and VWN–B–P potentials lead to similar results, indicating that the non-local corrections have only a small influence on $\Delta\omega$. From the data on CO/Cu, the SCF effects on the bond lengths and vibrational frequencies are small. Therefore the $\omega$ shifts are also similar for both perturbation and full SCF calculations.

For M = Ni, the calculated $d\omega_{C-O}/dF$ is $1.31 \times 10^{-6}$ or $1.43 \times 10^{-6}$ cm$^{-1}$ V$^{-1}$ cm. Lambert's more recent observed value for CO/Ni(100) is $(1.4 \pm 0.3) \times 10^{-6}$ cm$^{-1}$ V$^{-1}$ cm. The calculation and experiment are in good agreement. According to the calculations, the $d\omega_{C-O}/dF$ value exhibits a very slight decrease from M = Ni to M = Pt and from M = Cu to M = Au. The experimental UHV value of $(0.34 \pm 0.09) \times 10^{-6}$ cm$^{-1}$ V$^{-1}$ cm for CO/Pt(111)[15] is shown to be markedly (*ca.* four times) smaller than the calculated values. A more recent measurement[16] shows that the tuning rate for CO/Pt at a low coverage of CO would be higher, *ca.* $(7.5 \pm 0.9) \times 10^{-7}$ cm$^{-1}$ V$^{-1}$ cm. In any case, the measured $d\omega_{C-O}/dF$ value of CO on Pt in UHV is unexpectedly small in view of the experimental data in electrolytes as well as the UHV values for CO/Ni. One possible explanation[16] is that the actual electrostatic field across the CO adlayer is less than the measured average field between the electrodes in UHV. Further investigation is required to prove this argument.

The calculations give very similar results for M = Ni and Cu. The agreement is expected because the dynamic dipole moment $\mu$ is approximately equal for CO on Ni(100) and Cu(100).[14] Our calculated values are also in quite good agreement with the calculations of Bagus *et al.* for CO on Cu(100), which gave a tuning rate of $1.4 \times 10^{-6}$ cm$^{-1}$ V$^{-1}$ cm for the $Cu_{10}CO$ cluster.[19]

**Table 5** Frequency differences ($\Delta\omega$ in cm$^{-1}$) between the values for $F = 0$ and $F = \pm 0.01$ a.u.

| | | M—CO | | C—O | | |
|---|---|---|---|---|---|---|
| | | $\Delta\omega^{(1)a}$ | $\Delta\omega^{(2)b}$ | $\Delta\omega^{(1)}$ | $\Delta\omega^{(2)}$ | $d\omega^{av}/dF$ $10^6$ cm$^{-1}$ V$^{-1}$ cm |
| M = Ni | VWN | −4(−4) | −4(−6) | 67(67) | 68(71) | 1.31 |
| | VWN–B–P | −2 | −2 | 73 | 74 | 1.43 |
| M = Pd | VWN | −8(−12) | −5(−10) | 59(63) | 62(64) | 1.18 |
| | VWN–B–P | −9 | −7 | 70 | 75 | 1.41 |
| M = Pt | VWN | −9(−4) | −8(−4) | 56(71) | 58(75) | 1.11 |
| | VWN–B–P | −1 | 1 | 69 | 71 | 1.36 |
| M = Cu | VWN | −8(−5) | −8(−7) | 65(72) | 68(63) | 1.29 |
| | VWN–B–P | −17 | −14 | 65 | 69 | 1.30 |
| M = Ag | VWN | −9(−2) | −13(−5) | 62(70) | 65(73) | 1.24 |
| M = Au | VWN | 1(0) | −1(0) | 58(65) | 60(69) | 1.15 |

[a] $\Delta\omega^{(1)} = \omega(F = +0.01$ a.u.$) - \omega(F = 0)$. [b] $\Delta\omega^{(2)} = \omega(F = 0) - \omega(F = -0.01$ a.u.$)$. The values in parentheses are the non-relativistic results.

By conversion, the calculated VWN values correspond to 31–36 $cm^{-1}$ $V^{-1}$. The calculation with the VWN–B–P potential gives slightly larger values for the transition metals, 38–40 $cm^{-1}$ V. The experimental values shown in Table 1 vary from 30 to 60 $cm^{-1}$ $V^{-1}$, depending on the author, the metal and the electrolyte. The calculated values can be considered to agree qualitatively with the experimental data. However, it is not easy to give a 'quantitative' comparison of the calculated results with the experimental ones. The reasons are that (1) there are some uncertainties in the conversion factor from the experimental $\omega$ dependence on the applied voltage to the local electric field.[14,22,58] (2) The influence of the solvent is neglected in the calculations; it has been shown that different solvents may yield noticeably different $\omega_{C-O}$–$V$ slopes.[59] (3) The C—O frequencies are known to be sensitive to the overall CO coverage; this is also not considered in the calculations. The remarkable result here is that there is no obvious trend in the calculated $\Delta\omega_{C-O}$ among the metals. This is in accord with the experimental observation of Ikezawa *et al.*[10] From the experimental measurements of Kunimatsu *et al.*,[4,6,8] however, the frequency shift with potential $V$ for CO on Au is twice as large as that for CO on Pt, and the rate does not depend on the electrolyte. According to our calculations, the difference cannot be attributed to a difference in $d\omega/dF$. One explanation may be that the difference is caused by a difference in the structure of the double layer. However, the experimental results of Ikezawa *et al.*[10] do not show a difference in $d\omega/dV$ between Au and other metals (Pd, Pt). The question whether there is any variation of $d\omega/dV$ with the metal is still open.

The non-relativistic calculation shows an increase in the magnitude of $\Delta\omega$. For M = Pt, $\Delta^{rel}\Delta\omega$ is *ca.* $-15$ $cm^{-1}$ (26%). For the other metals, the relativistic effects on $\Delta\omega$ are small.

Recently, we carried out similar ADF calculations for $CN^-$ adsorbed on coinage metal electrodes (Cu, Ag, Au).[60] The vibrational tuning rates $d\omega_{C-N}/dF$ obtained are 5.6–6.6 $\times 10^{-7}$ $cm^{-1}$ $V^{-1}$ cm, a factor of two smaller than the calculated $d\omega_{C-O}/dF$ values. Experimental frequency shifts for $CN^-$ on coinage metal electrodes are *ca.* 30 $cm^{-1}$ $V^{-1}$,[1,21] which are also nearly a factor of two smaller than the experimental data of 50–60 $cm^{-1}$ $V^{-1}$ for CO on Ag and Au shown in Table 1.

Only small changes in the M—CO bond length and frequency can be induced by an applied electric field. However, the M—CO property values show field-dependent shifts opposite to those shown by the C—O ones. The same behaviour was also found in the semiempirical ASED calculations of Anderson *et al.*[18] So far, little is known about the vibrational spectra of the metal–CO surfaces in solution[61] owing to the difficulty in obtaining sufficient sensitivity for IR in the low-frequency region.

## 4 Conclusions

A theoretical comparative study has been carried out for vibrational frequency shifts of CO on various metal M(100) surfaces in the presence of a uniform electric field. The electric field causes large changes in the C—O frequency $\omega_{C-O}$. The calculated vibrational tuning rates $d\omega_{C-O}/dF$ are (1.1–1.4) $\times 10^{-6}$ $cm^{-1}$ $V^{-1}$ cm, in good agreement with Lambert's observed values for CO/Ni[14] and also consistent with the cluster calculations of Bagus *et al.*[19,20] for CO/Cu. The resulting estimates of the vibrational tuning rate with potential $V$ are 31–38 $cm^{-1}$ $V^{-1}$, comparable to experimental data of *ca.* 30 $cm^{-1}$ $V^{-1}$ obtained in electrolytes by most authors. A notable fact is that there is only very small variation of the calculated tuning rate with the metal. This is in agreement with the experimental results of Ikezawa *et al.*, who obtained very similar frequency shifts with potential $V$ on different metal electrodes. Our calculations, however, do not support the rather small UHV value for CO on Pt. The difference in the tuning rate between experiments in vacuum and electrolyte for CO/Pt is surprising. Further investigations are needed in order to understand the exceptional nature of CO/Pt in UHV.

This work was supported by the Natural Science Foundation of Fujian Province, P. R. China. We thank a referee for his constructive comments.

## References


1 K. Ashley and S. Pons, *Chem. Rev.*, 1988, **88**, 673.
2 K. Kunimatsu, *J. Phys. Chem.*, 1984, **88**, 2195.
3 B. Beden, A. Bewick and C. Lamy, *J. Electroanal. Chem.*, 1983, **148**, 147.
4 K. Kunimatsu, *J. Electroanal. Chem.*, 1983, **145**, 219.
5 J. W. Russel, M. Severson, K. Scanlon, J. Overend and A. Bewick, *J. Phys. Chem.*, 1983, **87**, 293.
6 K. Kunimatsu, W. G. Golden, H. Seki and M. R. Philpott, *Langmuir*, 1985, **1**, 245.
7 K. Kunimatsu, H. Seki, W. G. Golden, J. G. Gordon II and M. R. Philpott, *Surf. Sci.*, 1985, **158**, 596.
8 K. Kunimatsu, A. Aramata, H. Nakajima and H. Kita, *J. Electroanal. Chem.*, 1986, **207**, 293.
9 M. A. Tadayyoni and M. J. Weaver, *Langmuir*, 1986, **2**, 179.
10 Y. Ikezawa, H. Saito, H. Matsubayashi and G. Toda, *J. Electroanal. Chem.*, 1988, **252**, 395.
11 S-C. Chung, L-H. H. Leung and M. J. Weaver, *J. Phys. Chem.*, 1989, **93**, 5341.
12 D. K. Lambert, *Phys. Rev. Lett.*, 1983, **50**, 2106.
13 D. K. Lambert, *Solid State Commun.*, 1984, **51**, 297.
14 D. K. Lambert, *J. Chem. Phys.*, 1988, **89**, 3847; *Chem. Phys.*, 1991, **94**, 6237.
15 J. S. Luo, R. G. Tobin, D. K. Lambert, F. T. Wagner and T. E. Moylan, *J. Electron. Spectrosc. Relat. Phenom.*, 1990, **54/55**, 469.
16 J. S. Luo, R. G. Tobin and D. K. Lambert, *Chem. Phys. Lett.*, 1993, **204**, 445.
17 A. B. Anderson, R. Kötz and E. Yeager, *Chem. Phys. Lett.*, 1981, **82**, 130.
18 N. K. Ray and A. B. Anderson, *J. Phys. Chem.*, 1982, **86**, 4851; S. P. Mehandru and A. B. Anderson, *J. Phys. Chem.*, 1989, **93**, 2044.
19 P. S. Bagus, C. J. Nelin, W. Müller, M. R. Philpott and H. Seki, *Phys. Rev. Lett.*, 1987, **58**, 559.
20 P. S. Bagus, C. J. Nelin, K. Hermann and M. R. Philpott, *Phys. Rev. B*, 1987, **36**, 8169.
21 M. R. Philpott, P. S. Bagus, C. J. Nelin and H. Seki, *J. Electron. Spectrosc. Relat. Phenom.*, 1987, **45**, 169.
22 P. S. Bagus and G. Pacchioni, *Surf. Sci.*, 1990, **236**, 233.
23 P. S. Bagus and G. Pacchioni, *Electrochim. Acta*, 1991, **36**, 1669.
24 S. Holloway and J. K. Nørskov, *J. Electronanal. Chem.*, 1984, **161**, 193.
25 C. Korzeniewski and S. Pons, *J. Phys. Chem.*, 1986, **85**, 4153.
26 M. Head-Gordon and J. C. Tully, *Chem. Phys.*, 1993, **175**, 37.
27 ADF program package, version 2.0.1: E. J. Baerends, D. E. Ellis and P. Ros, *Chem. Phys.*, 1973, **2**, 41; G. te Velde and E. J. Baerends, *J. Comput. Phys.*, 1992, **99**, 84.
28 S. H. Vosko, L. Wilk and M. Nusair, *Can. J. Phys.*, 1980, **58**, 1200.
29 A. D. Becke, *Phys. Rev. A*, 1988, **38**, 3098.
30 J. P. Perdew, *Phys. Rev. B*, 1986, **33**, 8822.
31 B. G. Johnson, P. M. W. Gill and J. A. Pople, *J. Chem. Phys.*, 1993, **98**, 5612.
32 J. Li, G. Schreckenbach and T. Ziegler, *J. Am. Chem. Soc.*, 1995, **117**, 486; C. Heinemann, R. H. Hertwig, R. Wesendrup, W. Koch and H. Schwarz, *J. Am. Chem. Soc.*, 1995, **117**, 495.
33 T. Ziegler, V. Tschinke, E. J. Baerends, J. G. Snijders and W. Ravenek, *J. Phys. Chem.*, 1989, **93**, 3050.
34 S. Andersson and J. B. Pendry, *Phys. Rev. Lett.*, 1979, **43**, 363.
35 C. W. Bauschlicher Jr., *Chem. Phys. Lett.*, 1985, **118**, 307.
36 J. L. Andrés, M. Duran, A. Liedós and J. Bertán, *Chem. Phys.*, 1991, **151**, 37.
37 K. P. Huber and G. Herzberg, *Molecular Spectra and Molecular Structure*, Van Nostrand Reinhold, New York, 1979, vol. IV.
38 K. Hermann, P. S. Bagus and C. W. Bauschlicher, *Phys. Rev. B*, 1984, **30**, 7313.
39 K. Hermann, P. S. Bagus and C. J. Nelin, *Phys. Rev. B*, 1987, **35**, 9467.
40 G. Pacchioni and P. S. Bagus, *J. Chem. Phys.*, 1990, **93**, 1209.
41 G. Doyen and G. Ertl, *Surf. Sci.*, 1974, **43**, 197.
42 J. C. Bertolini and B. Tardy, *Surf. Sci.*, 1981, **102**, 131.

43 S. Andersson, *Solid State Commun.*, 1977, **21**, 75.
44 H. Conrad, G. Ertl, J. Koch and E. E. Latta, *Surf. Sci.*, 1974, **43**, 462.
45 R. J. Behm, K. Christman, G. Ertl, M. A. van Hove, P. A. Thiel and W. H. Weinberg, *Surf. Sci.*, 1979, **88**, L59.
46 A. M. Bradshaw and F. M. Hoffmann, *Surf. Sci.*, 1978, **72**, 513.
47 G. Ertl, M. Neumann and K. M. Streit, *Surf. Sci.*, 1977, **64**, 393.
48 A. M. Baro and H. Ibach, *J. Chem. Phys.*, 1979, **71**, 4812.
49 R. A. Shigeishi and D. A. King, *Surf. Sci.*, 1976, **58**, 379.
50 H. H. Krebs and H. Luth, *Appl. Phys.*, 1977, **14**, 337.
51 J. Pritchard, *J. Vacuum Sci. Technol.*, 1972, **9**, 895.
52 B. A. Sexton, *Chem. Phys. Lett.*, 1979, **63**, 451.
53 S. Andersson, *Surf. Sci.*, 1979, **89**, 477.
54 K. Horn and J. Pritchard, *Surf. Sci.*, 1976, **55**, 701.
55 C. J. Hirschmugl, Y. J. Chabal, F. M. Hoffmann and G. P. Williams, *J. Vac. Sci. Technol. A*, 1994, **12**, 2229.
56 M. Bowker, M. A. Barteau and R. J. Madix, *Surf. Sci.*, 1980, **92**, 528.
57 B. Beden, C. A. Melendres, G. A. Bowmaker, C. Q. Liu and V. A. Maroni, in *Synchrotron Techniques in Interfacial Electrochemistry*, ed. C. A. Melendres and A. Tadjeddine, Kluwer, Dordrecht, 1993.
58 A. B. Anderson, *J. Electroanal. Chem.*, 1990, **280**, 37.
59 S-C. Chang, X. Jiang, J. D. Roth and M. J. Weaver, *J. Phys. Chem.*, 1991, **95**, 5738; X. Jiang and M. J. Weaver, *Surf. Sci.*, 1992, **275**, 237.
60 M-S. Liao, X. Lü and Q-E. Zhang, *Int. J. Quantum Chem.*, in press.
61 Z-Q. Tian, B. Ren and B-W. Mao, *J. Phys. Chem.*, 1997, **101**, 1338.


*Paper* 7/06594I; *Received* 9*th September*, 1997